ELSEVIER

Materials Science and Engineering A261 (1999) 139–146

MATERIALS SCIENCE & ENGINEERING A

Dislocation processes during the deformation of $MoSi_2$ single crystals in a soft orientation

S. Guder [a,*], M. Bartsch [a], M. Yamaguchi [b], U. Messerschmidt [a]

[a] *Max Planck Institute for Microstructure Physics, Weinberg 2, Halle/Saale, D-06120, Germany*
[b] *Department of Materials Science and Engineering, Kyoto University, Kyoto, 606-01, Japan*

Abstract

In situ straining experiments in a high-voltage electron microscope have been carried out for the first time on $MoSi_2$ single crystals between 800 and 1000°C along a soft [201] orientation. Dislocations with $1/2\langle 111\rangle$Burgers vectors were formed in localised sources leading to almost planar slip. The dislocations were strictly arranged along 60° and edge orientations and moved at high velocities or in a viscous way. These observations are correlated to the macroscopic deformation behaviour and interpreted by the formation of intrinsic point defect atmospheres around the moving dislocations. The model explains the 'inverse' dependence of the strain rate sensitivity of the flow stress on the strain rate.

Keywords: Dislocation mobility; In situ straining experiments in a high-voltage electron microscope; $MoSi_2$; Strain rate sensitivity; Flow stress anomaly

1. Introduction

Because of its high melting point (2020°C), intermediate density, high thermal conductivity, good corrosion resistance and compatibility with ceramic reinforcements, $MoSi_2$ is a promising candidate material for structural high-temperature applications. However, it suffers from the disadvantages of most basic high-temperature materials, i.e. a low creep resistance at high temperatures and a low fracture toughness at room temperature. A prerequisite of tailoring composite materials is an understanding of the microprocesses of deformation of $MoSi_2$ single crystals. The high-temperature deformation properties have been investigated by several groups, a number of slip systems were identified (e.g. [1–5]) and dislocation reactions and dissociations have been proposed (e.g. [1–3,6,7]). $MoSi_2$ shows a strong plastic anisotropy and it was demonstrated in [3] that in soft orientations $MoSi_2$ can plastically be deformed down to room temperature. The $\{011\}\langle 100]$, $\{010\}\langle 100]$ and $\{110\}\langle 111\rangle$ slip systems exhibit a flow stress anomaly with a flow stress peak at about 850°C for the first two systems and at 1100°C for the latter one [3]. Between about 700 and 1000°C, the $\{110\}\langle 111\rangle$ system has by far the lowest critical flow stress. In spite of great achievements to clarify the slip processes, the mechanisms controlling the dislocation mobility are still open. The flow stress anomaly was interpreted either by locking owing to a dislocation dissociation on a cross slip plane [1] as in other intermetallics (e.g. [8]) or by the Portevin–Le Châtelier effect [3] due to interstitial impurities.

Recently, a straining stage for a high-voltage electron microscope (HVEM) has been designed for temperatures above 1000°C [9]. It allows direct observation of the dislocation motion and was successfully applied to brittle high-temperature materials (e.g. [10]). The present paper addresses the problems of the mechanisms controlling the dislocation mobility during the deformation of $MoSi_2$ single crystals by performing such in situ straining experiments between 800 and 1000°C. A [201] tensile direction was chosen as it implies a high orientation factor for the $\{110\}\langle 111\rangle$ slip system with a particularly low flow stress between 700 and 1000°C, as described above. A low flow stress of the specimens is decisive for the success of the in situ straining experiments, because of the brittleness of the material, even at the relatively high temperatures.

Macroscopic compression experiments were carried out in the same orientation but in a wider temperature

* Corresponding author.

0921-5093/99/$ - see front matter
PII: S0921-5093(98)01059-4

range to support the interpretation of the in situ experiments. They were aimed particularly at determining the strain rate sensitivity of the flow stress, which was measured only scarcely up to now. Macroscopic compression was also used to introduce a certain dislocation density into the starting material for preparing the specimens for the in situ experiments. This was necessary to prevent brittle fracture before plastic deformation.

2. Experimental

$MoSi_2$ single crystals were grown by the optical floating zone method as described previously [3]. Specimens for macroscopic testing of two different sizes, about $5 \times 2 \times 1$ mm^3 and $10 \times 2 \times 1$ mm^3, were cut by spark erosion, ground and polished. They had a [201] compression axis and (010) and ($\bar{1}$02) side faces.

Specimens for the in situ straining experiments were prepared either from as-received crystals or from compression samples deformed at a strain rate of 10^{-5} s^{-1} up to about 0.3–0.4% total strain at 1200°C. Slices were cut of about $8 \times 2 \times 0.3$ mm^3 in size with the same loading axis as the compression bars and (010) foil planes. Two holes 5 mm apart were drilled to fix the specimens to the straining stage. Afterwards, the samples were ground and polished with diamond paste to a thickness of about 100 μm, dimpled at the centre to a residual thickness of about 20–30 μm and ion-milled with Ar ions till perforation occurred.

The specimens were deformed in the high-temperature straining stage described in [9] inside an HVEM operated at 1000 kV. The experiments were performed between 800 and 1000°C. The load acting on the specimens is measured by semiconducting strain gauges and is usually increased by incremental steps. The straining stage allows the specimens to be tilted around two axes by about $\pm 10°$ in order to adjust suitable imaging conditions. The structures and the dynamic behaviour of dislocations were recorded either on photographic film or on video tape. The microstructure of the deformed specimens was usually characterised in detail by a post mortem analysis in the HVEM in a wide-angle goniometer at room temperature.

The macroscopic compression tests were carried out at a strain rate of 10^{-5} s^{-1} between 300 and 1200°C in a digitally controlled single screw testing machine at ambient atmosphere. The strain rate sensitivity of the flow stress was determined by stress relaxation tests. The stress relaxation curves were plotted as $\ln(-\dot{\sigma})$ versus σ. In this plot, the inverse slope $\Delta\sigma/\Delta\ln(-\dot{\sigma})$ yields the strain rate sensitivity r, according to

$$r = \Delta\sigma/\Delta\ln\dot{\varepsilon} = \Delta\sigma/\Delta\ln(-\dot{\sigma}). \quad (1)$$

During a relaxation curve, the actual strain rate $\dot{\varepsilon}$ decreases continuously. Thus, r can be measured as a function of the strain rate by taking several slopes along a single relaxation curve. The negative relaxation rates ($-\dot{\sigma}$) are converted to the actual strain rates $\dot{\varepsilon}$ by considering the stiffness of the specimen and the fixtures.

3. Results

3.1. In situ straining experiments in a high-voltage electron microscope

3.1.1. Procedure of in situ straining experiments

The first in situ experiments were performed on as-received single crystals at 800°C. All specimens broke in a brittle way. Nevertheless, dislocations and stacking faults on (001) planes had been formed in connection with the crack propagation. As the post mortem characterisation was only partly successful, these results are not described further.

Since the in situ deformation of as-received crystals did not allow recording of dislocation motion, specimens were prepared which were exposed to prior compression as described in Section 2. This predeformation was carried out to introduce a sufficient number of dislocations which can move during the successive in situ deformation. The induced dislocations show 1/2⟨111⟩ and ⟨100] Burgers vectors. The latter ones were arranged end-on. Compression tests confirmed that the ⟨100] dislocations were activated only above 1000°C.

In situ straining experiments where dislocation motion was observed were successfully carried out in a temperature range of 930–1000°C. It turned out that 1000°C is an upper limit for high-temperature in situ straining of $MoSi_2$ single crystals since above this temperature specimen degradation drastically reduces the observation time. Usually, the straining experiments began with several sudden load drops while the driving current of the tensile stage was incrementally increased. Thereafter, the specimens deformed continuously and the dislocation motion was recorded at increasing, constant or decreasing load.Stacking faults on (001) planes with fault vectors parallel to [001] are created during in situ experiments in an HVEM, with and without load. Their sudden generation and electron microscopy contrast suggest that they are formed by a dissociation of dislocations with 1/2⟨111⟩ Burgers vectors by glide of dislocations with 1/2⟨110] Burgers vectors on (001) planes. The appropriate results are not in agreement with [7,11,12] and will be discussed in a future work.

3.1.2. Dislocation generation

After the serrations recorded during loading the specimens in the in situ straining experiments, usually a

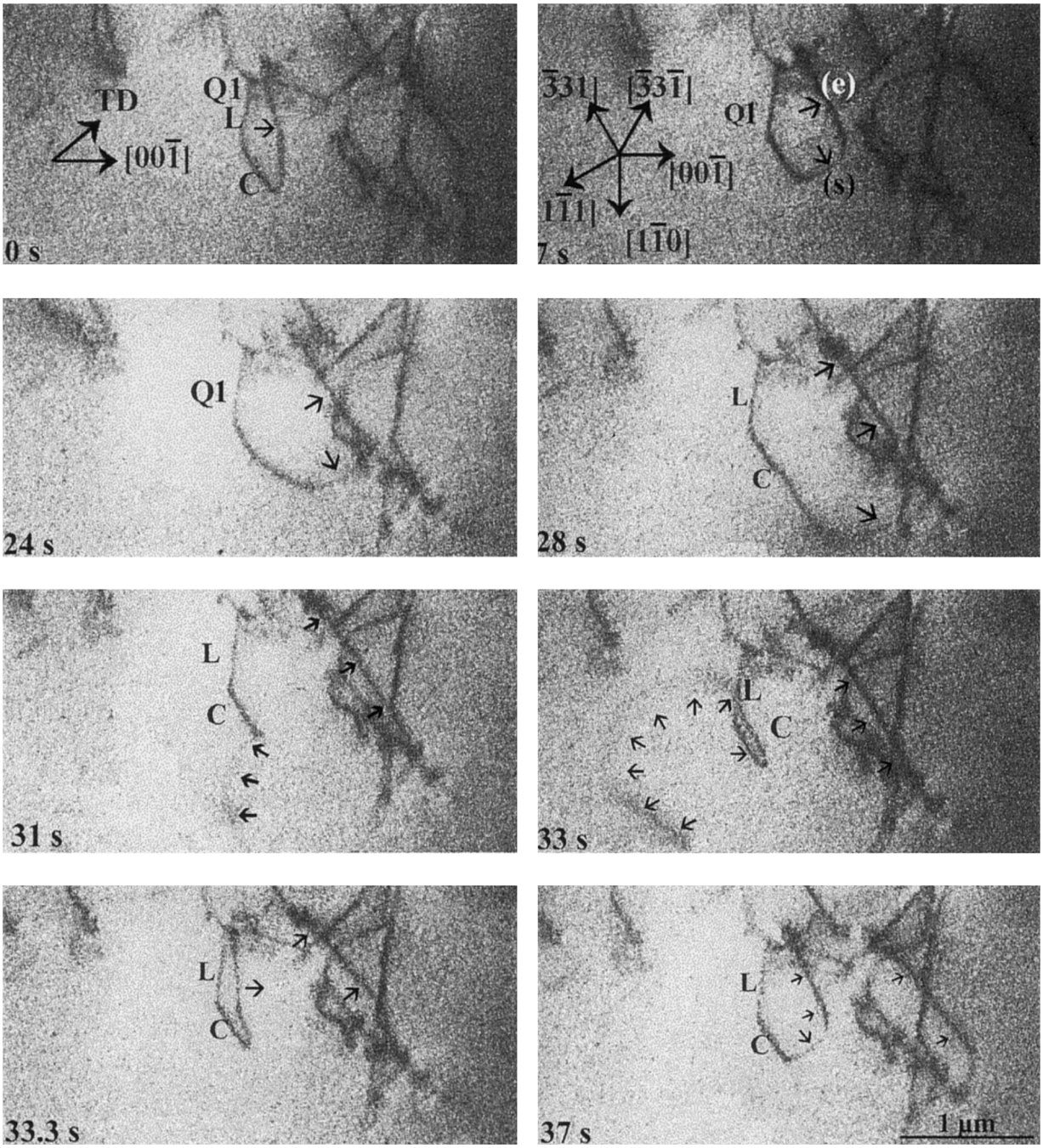

Fig. 1. Video sequence of a localised single-ended dislocation source Q1 generating dislocations with 1/2[1$\bar{1}$1] Burgers vector on parallel (110) planes during straining along [201] (TD, tensile direction) at 1000°C and viewed along [010]. Segment L on the (110) slip plane is aligned along [1$\bar{1}$0], segment C is probably on another plane. Arrows mark the mobile arm of the source, (e) and (s) indicate edge and screw segments of the mobile arm. Crystallographic directions on (110) planes are inserted which for a dislocation with 1/2[1$\bar{1}$1] Burgers vector represent 30, 60 and 90° character, respectively.

small number of slip bands was detected. In all cases analysed these dislocations had 1/2⟨111⟩ Burgers vectors and were moving on {110) planes. Since these dislocations were formed during the sudden load drops, they must have moved at very high velocities. Later on, during continuous deformation, the operation of a source of dislocations with 1/2⟨111⟩ Burgers vector was recorded on video tape. Some stages are shown in Fig. 1. The source labelled Q1 consists of one segment on the primary (110) slip plane and oriented along [1$\bar{1}$0] labelled L, a second segment labelled C probably in another slip plane and therefore having a low mobility, and a mobile arm marked by arrows. This arm bows out under load and emits new dislocations on parallel

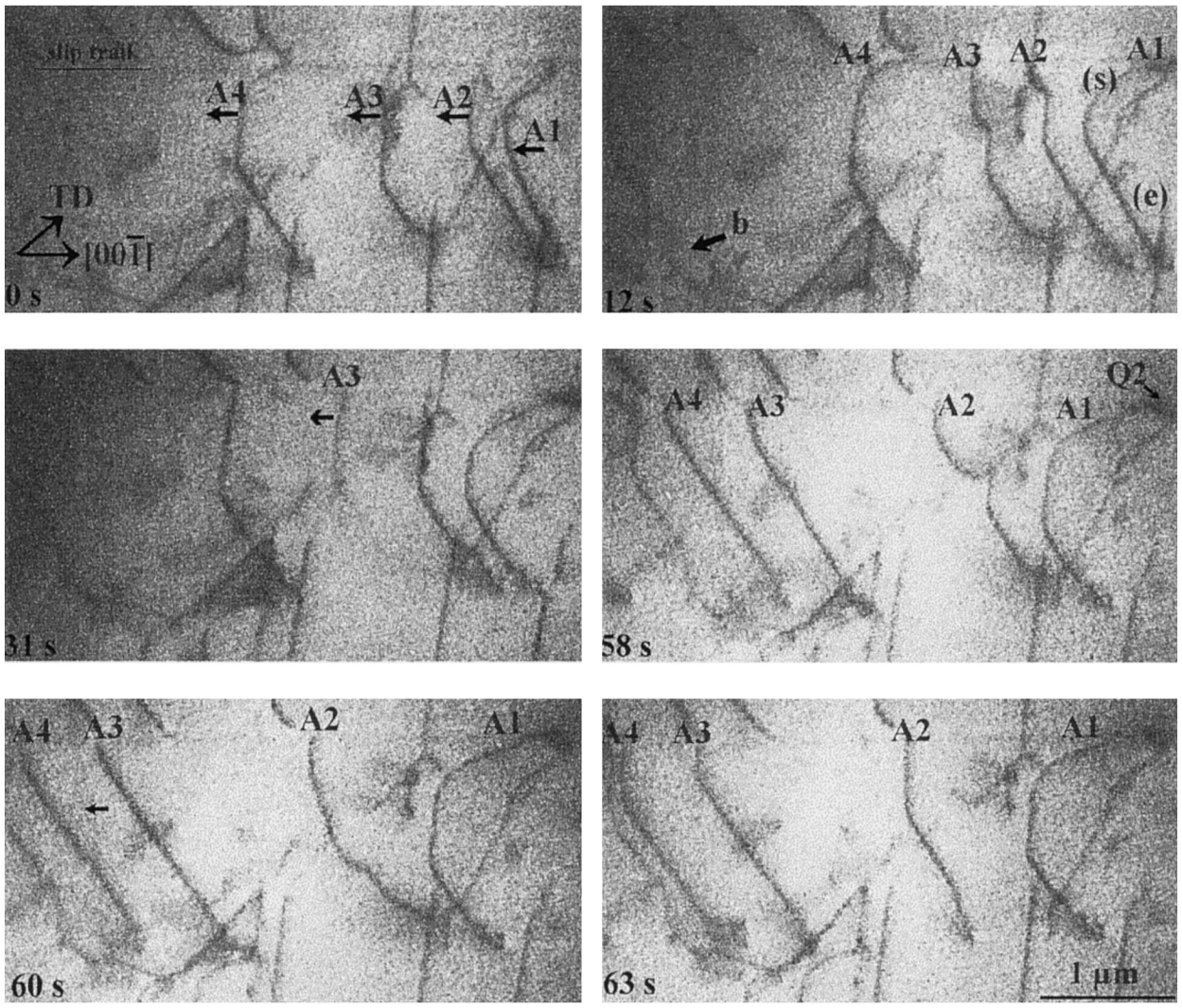

Fig. 2. Video sequence of mobile 1/2[1$\bar{1}$1] dislocations (marked as A1–A4) on parallel (110) planes during straining along [201] (TD, tensile direction) at 1000°C and viewed along [010]. Slip trails of the 1/2[1$\bar{1}$1] dislocations run parallel to the [001] direction. A surface-near dislocation source is marked by Q2, screw and edge segments are marked by (s) and (e), respectively. Direction of motion and Burgers vector are indicated by arrows.

(110) planes. Thereby the mobile arm prefers edge and screw orientation, as marked in Fig. 1 by (e) and (s), respectively. After intersecting the foil plane the mobile arm moves very fast (Fig. 1 at 31–33.3 s). The dislocation emitted towards the left side moves quickly while that emitted towards the right side interacts with other dislocations and moves therefore at a rather low velocity (compare its positions in Fig. 1 at 33 and 37 s). This type of single-ended source emits dislocations on the same or neighboured slip planes, leading to planar slip or very narrow slip bands.

3.1.3. Dislocation motion

Once generated, the dislocations with 1/2⟨111⟩ Burgers vectors can move easily on their {110) planes over long distances at high velocities. They stop near groups of other dislocations or move in a viscous way at lower velocities. Thus, the dislocations may experience a low friction at high velocities and long-range interaction forces are important, in addition to the processes controlling the dislocation mobility. Fig. 2 shows some stages of the motion of 1/2[1$\bar{1}$1] dislocations taken from a video recording. The characteristic feature is their preferential orientation along [1$\bar{1}$0] and [$\bar{3}$31] (60° and edge character). Resting dislocations analysed post mortem at room temperature still exhibit these 60 and 90° characters. When moving at high velocities dislocations prefer 60° character. At lower velocities they orient along both 60° and edge orientation (e.g. dislocations A2 to A4 in Fig. 2 at 0 s) or exhibit pure edge character (e.g. dislocations A3 and A4 in Fig. 2 at 58 s). Their motion appears either by shifting superkinks (e.g. dislocation A2 and A3 in Fig. 2 at 12 s) or by taking a curved shape (e.g. dislocation A2 in Fig. 2 at 60 s). A

dislocation labelled A1 is generated by a source Q2 near the foil surface. Its screw segment (s) bows out very slowly on its glide plane, showing that it does not exhibit a high mobility.

Cross slip on {011) planes containing the same Burgers vector has never been observed by in situ straining or by post mortem analysis.

3.2. Results of macroscopic compression tests

Macroscopic compression tests were performed to supplement the results of the in situ straining experiments. Fig. 3 shows stress–strain curves obtained from $MoSi_2$ single crystals compressed along [201] at temperatures between 300 and 1200°C at a strain rate of 10^{-5} s^{-1}. The crystals exhibit an anomalous increase of the flow stress with increasing temperature in an intermediate temperature range between 600 and 1000°C and a normal decrease at lower and higher temperatures. The range of anomaly can exclusively be attributed to the {110)⟨111⟩system since a slip trace analysis confirmed a further slip system only at temperatures above 1000°C. The range of anomaly coincides with serrated yielding and coarse slip bands observed macroscopically. Here, the stress before a load drop occurs is independent of the strain rate of deformation.

Stress relaxation tests were carried out at each deformation temperature and were analysed except those for 750°C. At this temperature almost no stress relaxation was measured after serrated yielding. Fig. 4 shows some stress relaxation curves plotted as $\ln(-\dot{\sigma})$ versus σ. As described in Section 2, the inverse slope of these curves equals the strain rate sensitivity r. $MoSi_2$ single crystals which were compressed at 300°C and above 1000°C show 'normal' relaxation curves, i.e. the curves are bent towards the stress axis so that the strain rate sensitivity increases with increasing stress or strain rate. This corresponds to the smooth stress–strain curves in Fig. 3. With an increasing tendency to localised slip, the strain rate sensitivity decreases towards very small values (above 400°C) and the shape of the relaxation curves changes to an 'inverse' curvature when serrations determine the macroscopic deformation behaviour, e.g. at 940°C. The dependence of the strain rate sensitivity on the strain rate is determined from the different slopes along the individual relaxation curves, as described in Section 2. These data are summarised in Fig. 5 which demonstrates the 'usual' behaviour of rising curves outside the anomalous temperature range and falling curves within it.

4. Discussion

In the present experiments, deformation along a [201] direction activated dislocations on the {110)⟨111⟩ slip system. The temperature dependence of the flow stress for the {110)⟨111⟩ slip system is qualitatively similar to that expected from [2,3,5]. The interpretation of the results is concentrated on the temperature range where the in situ experiments were performed, i.e. on the range of flow stress anomaly of the {110)⟨111⟩ slip system.

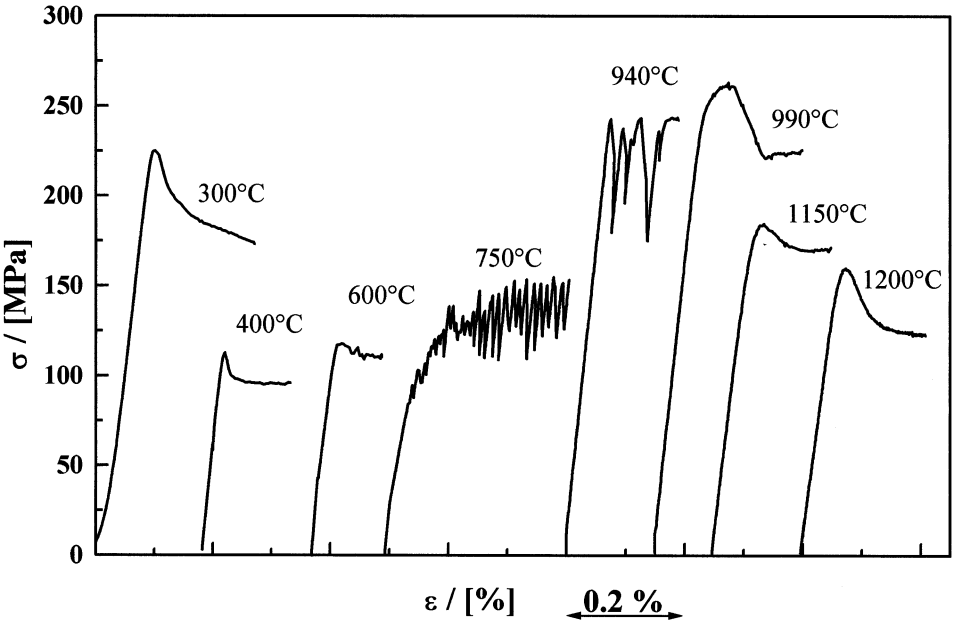

Fig. 3. Stress–strain curves of $MoSi_2$ with a [201] compression axis deformed at different temperatures at a strain rate of 10^{-5} s^{-1}.

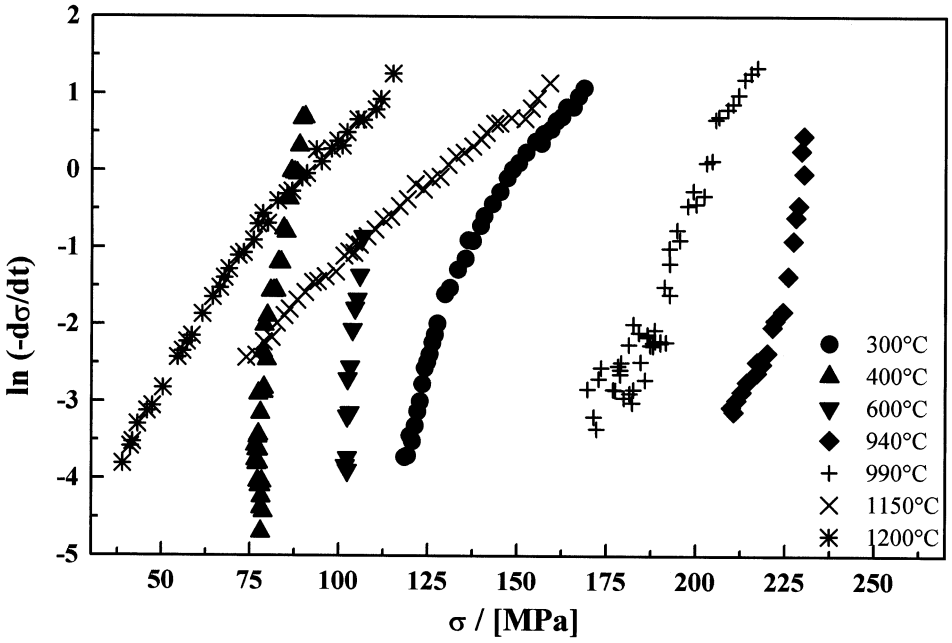

Fig. 4. Stress relaxation curves at different temperatures and approximately equal strain of 0.2%.

4.1. Dislocation generation

During the in situ experiments, glide dislocations with $1/2\langle 111\rangle$ Burgers vectors were created very instantaneously during the load drops at first loading the specimens and continuously from localised sources during subsequent continuous deformation, as described in Section 3.1.2. The activation of localised sources, i.e. sources which operate repeatedly and thus emit a greater number of dislocations on the same or neighbouring slip planes, indicates that cross slip on possible {011} planes is difficult. Only few localised sources emitting a great number of dislocations yields very narrow slip bands, which can be correlated to the individual serrations in the macroscopic stress–strain curves. An inhomogeneous distribution of dislocations in bundles was also observed by conventional transmission electron microscopy [3].

4.2. Alignment of dislocations with $1/2\langle 111\rangle$ Burgers vector

As described in Section 3.1.3, an outstanding feature of dislocations with $1/2\langle 111\rangle$ Burgers vectors under stress is their strict arrangement along crystallographic orientations. The observed $\langle 110]$ and $\langle 331]$ directions correspond to the 60° and edge characters, respectively. Preference orientations were already observed by conventional transmission electron microscopy, however less strictly expressed: the $\langle 110]$ (60°) orientation between 1000 and 1200°C in [2,3,7] and for polycrystalline $MoSi_2$ between 600 and 1000°C in [5]. A preferred edge orientation has not been observed before at temperatures between 800 and 1000°C.

Preferred orientations of dislocations may be an expression of anisotropic line tension. However, the dependence of dislocation line energy on the orientation calculated in [13] does not indicate strong effects of the elastic anisotropy on the shape of bowing segments.

The strict preference of some orientations is certainly a core property and corresponds to deep energy valleys. As the dislocations change their shape during motion, either by suppressing one of the preferred orientations, or by getting curved, or by forming superkinks, the preferred orientations seem to express minima of the dislocation energy. Thus, the Peierls stress, which may be responsible for the low-temperature increase of the flow stress, is still active in the range of the flow stress anomaly.

4.3. Dislocation dynamics/model

It is a unique advantage of the in situ straining experiments to yield information on the dynamic behaviour of the dislocations. As described in Section 3.1.3, there is no indication of extrinsic defects impeding the dislocation motion in the range of the flow stress anomaly. However, there exists a coexistence of dislocation motion at high velocities, pointing to a low friction, and a viscous motion at low velocities. This feature fits a model which explains the dynamic dislocation properties as well as the occurrence of a flow stress anomaly by the formation of point defect atmospheres, in addition to the Peierls mechanism.

The $MoSi_2$ single crystals show a particular dependence of the strain rate sensitivity r on the strain rate $\dot{\varepsilon}$, as demonstrated in Fig. 5. At low and high tempera-

tures, r increases with increasing $\dot{\varepsilon}$, which is characteristic of usual obstacle mechanisms. The opposite behaviour is observed in the range of the flow stress anomaly. This can easily be explained by the formation of point defect atmospheres in this temperature range, leading to strain ageing effects. This interpretation is in accordance with [3], where the Portevin–Le Châtelier effect was discussed as a probable mechanism of the flow stress anomaly in $MoSi_2$. As reviewed in [14], atmospheres of different origin yield an increasing contribution to the flow stress with increasing dislocation velocity or strain rate in the range of low velocities. Then, the stress reaches a maximum and decreases slowly at higher velocities. The slope of the stress versus $\ln \dot{\varepsilon}$ curve is identical with the contribution of this process to the strain rate sensitivity of flow stress. The latter is high at small strain rates and decreases down to zero at the maximum stress. At higher strain rates, the strain rate sensitivity becomes negative. The 'inverse' behaviour at low strain rates is shown in the curves for 940 and 990°C of Fig. 5. Similar effects were also observed in TiAl [15].

This macroscopic behaviour is a consequence of the dynamic properties of dislocations. As described in Section 3.1.3, very fast as well as slowly moving dislocations were observed at the same load of the specimen. This is certainly influenced by long-range stress fields, but it can well be explained by point defect atmospheres, as always two dislocation velocities belong to each stress. Thus, the localised generation of dislocations results in the inhomogeneity of slip while the dynamic dislocation behaviour with a low friction at high velocities results in the very fast load drops during the serrations.

Usually, strain ageing effects are caused by interstitial impurities as assumed also for $MoSi_2$ [3]. It is reviewed in [16] and follows from estimations using the formulae in [14] that impurity concentrations greater than 1000 ppm are necessary to yield an appreciable contribution of atmospheres to the flow stress. However, the interstitial impurity concentrations of the present crystals should be in the range of 300 wt ppm [3] and thus do not affect the flow stress in the anomalous range. A new model was proposed in [15] suggesting that the lowest energy configuration of the dislocation core in intermetallics may contain a certain concentration of intrinsic point defects, vacancies in one or both sublattices or antisite defects. When the dislocation moves, it has to drag this atmosphere. This process will lead to the same effects as other types of atmospheres, a flow stress anomaly and serrated yielding. However, this is an intrinsic effect, independent of impurities, which, in principle, may occur in all intermetallic alloys. In the anomalous range, the dislocations have their lowest mobility. Thus, the dislocation density has to be high in order to accommodate for the imposed strain rate. Consequently, a high athermal component of the flow stress, observed experimentally, does not contradict the model of intrinsic atmospheres

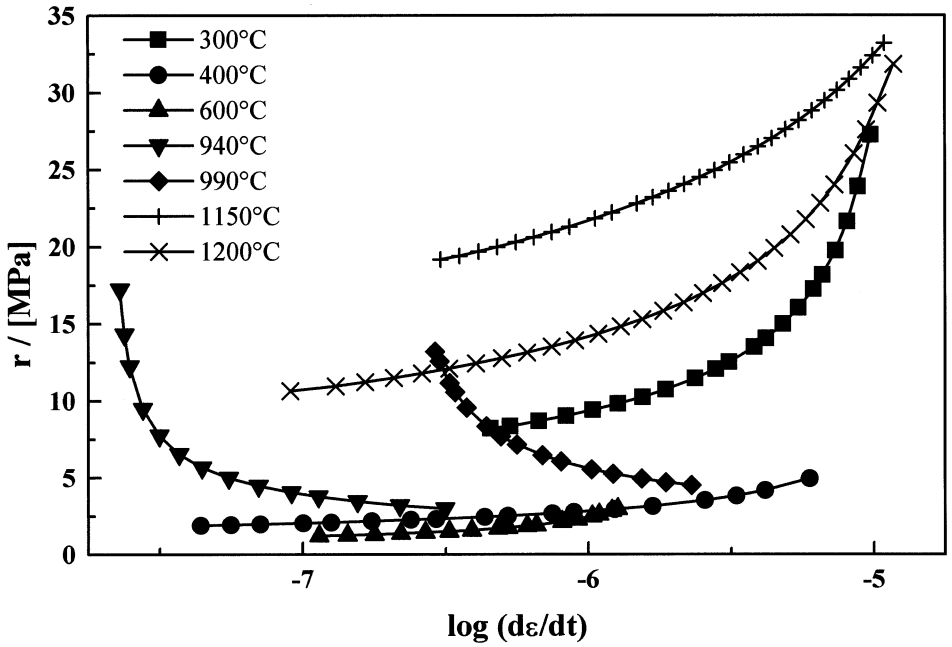

Fig. 5. Dependence of the strain rate sensitivity r on the logarithm of the strain rate $\dot{\varepsilon}$ with the temperature as parameter.

controlling the mobility of dislocations. Of course, additional experimental and theoretical work is necessary to discuss the model further.

5. Conclusions

Glide dislocations with $1/2\langle 111\rangle$ Burgers vectors are generated by localised sources emitting a greater number of dislocations on the same or neighbouring glide planes, in accordance with very high slip steps produced during serrated flow in the anomalous temperature range. These dislocations move either at high velocities or in a viscous way. They are arranged preferentially along 60° and edge orientations, which is certainly due to particular structures of the dislocation cores.

The occurrence of the flow stress anomaly and the dynamic dislocation behaviour can be explained by the formation of intrinsic point defect atmospheres, which may form if the lowest energy configuration of a dislocation in an intermetallic compound requires a certain concentration of intrinsic point defects, and which have to be dragged with the moving dislocations. This model is in agreement with the 'inverse' behaviour of the strain rate sensitivity of the flow stress in the anomalous temperature range.

References

[1] Y. Umakoshi, T. Sakagami, T. Hirano, T. Yamane, Acta Metall. Mater. 38 (6) (1990) 909.
[2] T.E. Mitchell, S.A. Maloy, Critical Issues in: N.S. Stoloff, D.J. Duquette, A.F. Giamei (Eds.), The Development of High Temperature Structural Materials, The Minerals, Metals and Materials Society, Warrendale, 1993, p. 279.
[3] K. Ito, H. Inui, Y. Shirai, M. Yamaguchi, Phil. Mag. A 72 (4) (1995) 1075.
[4] K. Kimura, M. Nakamura, T. Hirano, J. Mater. Sci. 25 (1990) 2487.
[5] S.A. Maloy, A.H. Heuer, J.J. Lewandowski, T.E. Mitchell, Acta Metall. Mater. 40 (11) (1992) 3159.
[6] D.J. Evans, S.A. Court, P.M. Hazzeldine, H.L. Fraser, Phil. Mag. Let. 67 (5) (1993) 331.
[7] S.A. Maloy, T.E. Mitchell, A.H. Heuer, Acta Metall. Mater. 43 (1995) 657.
[8] V. Paidar, D.P. Pope, V. Vitek, Acta Metall. 32 (1984) 435.
[9] U. Messerschmidt, M. Bartsch, Ultramicroscopy 56 (1994) 163.
[10] B. Baufeld, D. Baither, U. Messerschmidt, M. Bartsch, H. Foitzik, M. Rühle, J. Am. Ceram. Soc. 80 (7) (1997) 1699.
[11] B.K. Kad, K.S. Vecchio, R.J. Asaro, Phil. Mag. A 72 (1) (1995) 1.
[12] K. Ito, T. Nakamoto, H. Inui, M. Yamaguchi, MRS Symp. Proc. 460 (1997) 599.
[13] M. Nakamura, S. Matsumoto, T. Hirano, J. Mater. Sci. 25 (1990) 3309.
[14] J.P. Hirth, J. Lothe, Theory of Dislocations, Wiley, New York, 1982.
[15] U. Messerschmidt, M. Bartsch, S. Guder, D. Häußler, R. Haushälter, M. Yamaguchi, Intermetallics, to be published.
[16] L.P. Kubin, Y. Estrin, J. Phys. III (1) (1991) 929.